
A stochastic finite element procedure for moment and reliability analysis

Bruno Sudret* — Marc Berveiller*,** — Maurice Lemaire**

* *Electricité de France - R&D Division, Site des Renardières
F-77818 Moret-sur-Loing*

** *LaMI - UBP & IFMA
Institut Français de Mécanique Avancée
Campus de Clermont-Ferrand - Les Cézeaux, BP 265, F-63175 Aubière
{bruno.sudret, marc.berveiller}@edf.fr
maurice.lemaire@ifma.fr*

ABSTRACT. A new stochastic finite element procedure (SFEP) in the tradition of Ghanem's work is presented. It allows to deal with any number of input random variables of any type that can model both material properties and loading. The method makes use of Hermite series expansion of the input random variables and polynomial chaos expansion of the response, for which an original implementation is proposed. The link with reliability analysis is also established. Three application examples in geotechnical engineering are given for the sake of illustration. The accuracy and efficiency of SFEP is thoroughly investigated by comparison with well-established approaches.

RÉSUMÉ. On présente ici une nouvelle procédure aux éléments finis stochastiques baptisée SFEP. Elle permet de traiter des problèmes où l'aléa, portant sur les propriétés matériau et le chargement, est représenté par des variables aléatoires de n'importe quel type et en nombre quelconque. On utilise le développement des variables aléatoires d'entrée en séries d'Hermite et le développement de la réponse sur le chaos polynomial, pour lequel une implémentation est proposée. On montre également comment exploiter les résultats pour faire de la fiabilité des structures. Trois exemples d'application en géomécanique sont présentés. La précision et l'efficacité de la méthode sont évaluées sur ces exemples par comparaison avec des méthodes standard.

KEYWORDS: stochastic finite elements, polynomial chaos, finite element reliability, parametric study, foundation.

MOTS-CLÉS : éléments finis stochastiques, chaos polynomial, fiabilité des structures, étude paramétrique, fondation.

1. Introduction

The so-called *stochastic finite element analysis* has been paid much attention in the past two decades. All the methods found in the literature under this denomination have the following common characteristics:

- a finite element model, *i.e.* the discretized version of the equations governing a physical phenomenon such as solid mechanics, heat transfer, etc.;
- a probabilistic model of the input parameters: random variables and/or random fields are introduced for this purpose.

Apart from these common points, the methods referred to as *stochastic finite element analysis* are rather different in nature. According to Sudret and Der Kiureghian (Sudret *et al.*, 2000), they may be classified as follows (see also (Schuëller, G. (Editor), 1997, Matthies *et al.*, 1997, Kleiber, M. (Editor), 1999) for general reviews on the topic and (Frangopol D.M., Maute K. (Editors), 2004) for recent advances):

- *second moment methods*: these methods essentially aim at computing the variations of the mechanical response around its mean value, *i.e.* they provide the mean and standard deviation of response quantities such as displacements or stresses. The *perturbation method* applied by (Hisada *et al.*, 1981; 1985, Liu *et al.*, 1986a; 1986b, Kleiber *et al.*, 1992) falls within this category. So does the *weighted integral method* proposed by (Deodatis, 1991, Deodatis and Shinozuka, 1991, Takada, 1991a; 1991b);

- *reliability methods*: these methods aim at computing the probability of failure of a mechanical system with respect to a failure criterion represented by a limit state function (Ditlevsen *et al.*, 1996). In the context of finite element analysis, the pioneering work by (Der Kiureghian *et al.*, 1983; 1988) has been followed by many contributions, e.g. (Lemaire, 1998, Lemaire *et al.*, 2000, Sudret and Der Kiureghian, 2002). The so-called *finite element reliability methods* are nowadays applied in various industrial contexts, e.g. (Frangopol and Imaia, 2000, Imaia and Frangopol, 2000, Pendola *et al.*, 2000, Mohamed *et al.*, 2002, Sudret *et al.*, 2005);

- *polynomial chaos expansion methods (PCEM)*: these methods aim at representing the full probabilistic content of the mechanical response as a polynomial series expansion in standard normal variables. In this respect, PCEM provide an *intrinsic* representation of the response, since each response quantity is characterized as a random variable through expansion coefficients. The spectral stochastic finite element method (SSFEM) proposed by Ghanem and Spanos pertains to this category. This representation can be used together with Monte Carlo simulation to obtain the probability density function (PDF) of response quantities or second moment information. The use of SSFEM for finite element reliability analysis has also been demonstrated by Sudret and Der Kiureghian (Sudret *et al.*, 2002).

The present paper is related to this third category of so-called stochastic finite element methods denoted hereinafter by PCEM. Before detailing its objectives, a rapid review of the specific literature is necessary. The original work by (Ghanem and Spanos, 1990; 1991) deals with linear stochastic boundary value problems in which

the spatial variability of a material property (e.g. Young's modulus) is modeled using a random field, which is discretized using the Karhunen-Loève expansion. Later on, the same approach has been applied to transport in porous media (Ghanem, 1998), heat transfer (Ghanem, 1999b, Xiu *et al.*, 2003) and recently soil-structure interaction (Ghiocel *et al.*, 2002) and structural dynamics (Van Den Nieuwenhof *et al.*, 2003).

In all these applications, the spatial variability of one or more material properties is represented by a Gaussian or lognormal random field. Attempts to applying the approach to non linear problems can be found in Anders and Hori (Anders *et al.*, 1999, Anders *et al.*, 2001) (bounds on the solution are derived) as well as in Keese and Matthies (Keese *et al.*, 2002). A general framework for stochastic mechanics based on these ideas is described by (Ghanem, 1999a). Babuska *et al.* propose a similar framework and discuss convergence issues and error estimators (Deb *et al.*, 2001, Babuska *et al.*, 2002).

In the spirit of many of these papers, the use of polynomial chaos expansion in order to represent the stochastic mechanical response is related to spatial variability and the use of random fields. It is clear though that the use of the polynomial chaos expansion is only a way of representing the mechanical response. It should be independent from the way the input uncertainties is represented. Moreover, most applications in engineering mechanics are concerned with modeling the uncertainties in model parameters by using random variables instead of random fields. Indeed, the spatial fluctuations of a parameter are often second-order quantities compared to the uncertainty of the parameter considered as homogeneous (geomechanics may be in some cases a remarkable exception).

Of course, random variables may be considered as the limit case of random fields having infinite correlation length. However, the formalism proposed in the papers presented above is not directly suitable to this situation. Indeed, the random variables used for instance in structural reliability may have various types of distribution (not only Gaussian or lognormal), they may be correlated. What is more, loading is often the principal source of randomness and is rarely taken into account in the above references (although the possibility of having random loading is mentioned e.g. in (Ghanem *et al.*, 1991)). Finally, most papers do not address the problems related to post-processing. Their application examples are often limited to the presentation of the expansion coefficients of the principal unknowns (e.g. nodal displacement, temperature), sometimes mean and standard deviation of those. The inattentive reader can then wonder about the point of such complex methods if only mean and standard deviation of response quantities (which may be obtained easily by crude Monte Carlo simulation) are sought for. In other words, the great potential of these PCEM methods is scarcely fully taken advantage of. As a consequence of these observations, the present paper aims at:

- developing a new framework for stochastic finite element analysis, which allows to take into account any number of random variables of any type to model the input uncertainties. Thus random Young's modulus, Poisson's ratio, initial stress state and loading may be considered in the analysis. An original implementation of the

polynomial chaos used to represent the stochastic response and related tools are also presented;

- deriving useful relationships in order to expand strain or stress response quantities onto the polynomial chaos;
- developing the specific post-processing for moment analysis (*i.e.* computing the first four moments of the response), reliability analysis and PDF representation;
- comparing different numerical solving schemes in terms of accuracy and computational efficiency on application examples, in order to conclude about the “good practices” in stochastic finite element analysis.

The proposed *stochastic finite element procedure* (SFEP) presented in the sequel requires expanding the input random variables (or functions thereof) as Hermite series of standard normal random variables. This is detailed in Section 2. SFEP is then presented in Section 3. The various possible post-processings are then described in Section 4. Finally three application examples in geotechnical engineering illustrate the method.

2. Hermite series expansion of random variables

2.1. Introduction and notation

Let us denote by $\mathcal{L}^2(\Theta, F, P)$ the Hilbert space of random variables with finite variance. Let us consider a random variable X with prescribed probability density function (PDF) $f_X(x)$ and cumulative distribution function (CDF) $F_X(x)$. The mathematical expectation is denoted by $E[\cdot]$. The expectation of a function $g(X)$ is defined by:

$$E[g(X)] = \int_{-\infty}^{\infty} g(x)f_X(x)dx \quad [1]$$

Let us denote by ξ a standard normal variable, $\varphi(x) = \frac{1}{\sqrt{2\pi}}e^{-\frac{x^2}{2}}$ the standard normal PDF and Φ the standard normal CDF. Let $\{H_i, i = 0, \dots, \infty\}$ be the Hermite polynomials defined by:

$$H_i(x) = (-1)^i \frac{1}{\varphi(x)} \frac{d^i \varphi(x)}{dx^i} \quad [2]$$

The set $\{H_i, i = 0, \dots, \infty\}$ is an orthogonal basis of the Hilbert space $\mathcal{L}^2(\varphi)$ of the square integrable functions with respect to the Gaussian measure (Malliavin, 1997). Thus:

$$E[H_i(\xi)H_j(\xi)] = \delta_{ij} \cdot i! \quad [3]$$

where δ_{ij} is the Kronecker symbol. Classical results (e.g. (Malliavin, 1997)) allow to expand any random variable X with prescribed PDF as a Hermite polynomial series expansion:

$$X = \sum_{i=0}^{\infty} a_i H_i(\xi) \tag{4}$$

where $\{a_i, i = 0, \dots, \infty\}$ are coefficients to be evaluated. Two methods are now presented for this purpose.

2.2. Computation of the expansion coefficients

2.2.1. Projection method

This method was used by (Puig *et al.*, 2002, Xiu and Karniadakis, 2002, Field and Grigoriu, 2004). Due to the orthogonality of the Hermite polynomials with respect to the Gaussian measure, it comes from Equation [4]:

$$E[X H_i(\xi)] = a_i E[H_i^2(\xi)] \tag{5}$$

where $E[H_i^2(\xi)] = i!$. By using the transformation to the standard normal space $X \rightarrow \xi: F_X(X) = \Phi(\xi)$, one can write:

$$X(\xi) = F_X^{-1}(\Phi(\xi)) \tag{6}$$

Thus:

$$a_i = \frac{1}{i!} E[X(\xi) H_i(\xi)] = \frac{1}{i!} \int_{\mathbb{R}} F_X^{-1}(\Phi(t)) H_i(t) \varphi(t) dt \tag{7}$$

When X is a normal, lognormal or uniform random variable, coefficients $\{a_i, i = 0, \dots, \infty\}$ can be evaluated analytically:

$$\begin{aligned} X \equiv N(\mu, \sigma) & \quad a_0 = \mu, a_1 = \sigma, a_i = 0 \quad \text{for } i \geq 2 \\ X \equiv LN(\lambda, \zeta) & \quad a_i = \frac{\zeta^i}{i!} \exp[\lambda + \frac{1}{2}\zeta^2] \quad \text{for } i \geq 0 \\ X \equiv U[a, b] & \quad a_0 = \frac{a+b}{2}, a_{2i} = 0, \\ & \quad a_{2i+1} = \frac{(-1)^i (b-a)}{2^{2i+1} \sqrt{\pi} i! (2i+1)} \end{aligned} \tag{8}$$

For other types of distribution, the integral in Equation [7] can be evaluated numerically using Gaussian quadrature (Sudret *et al.*, 2003).

2.2.2. Regression method

This method was introduced by (Webster *et al.*, 1996) and (Isukapalli, 1999). It is based on a least square minimization of the discrepancy between the input variable X and its truncated approximation \tilde{X} :

$$\tilde{X} = \sum_{i=0}^p a_i H_i(\xi) \quad [9]$$

Let $\{\xi^{(1)}, \dots, \xi^{(n)}\}$ be n outcomes of ξ . Equation [6] (resp. [9]) yields n outcomes $\{X^{(i)}, i = 1, \dots, n\}$ (resp. $\{\tilde{X}^{(i)}, i = 1, \dots, n\}$). The least square method consists in minimizing the following quantity with respect to $\{a_i, i = 0, \dots, p\}$:

$$\begin{aligned} \Delta X &= \sum_{i=1}^n (X^{(i)} - \tilde{X}^{(i)})^2 \\ &= \sum_{i=1}^n \left(F_X^{-1}(\Phi(\xi^{(i)})) - \sum_{j=0}^p a_j H_j(\xi^{(i)}) \right)^2 \end{aligned} \quad [10]$$

This leads to the following linear system yielding the expansion coefficients $\{a_i, i = 0, \dots, p\}$:

$$\begin{aligned} &\begin{pmatrix} \sum_{i=1}^n H_0(\xi^{(i)})H_0(\xi^{(i)}) & \cdots & \sum_{i=1}^n H_0(\xi^{(i)})H_p(\xi^{(i)}) \\ \vdots & \ddots & \vdots \\ \sum_{i=1}^n H_p(\xi^{(i)})H_0(\xi^{(i)}) & \cdots & \sum_{i=1}^n H_p(\xi^{(i)})H_p(\xi^{(i)}) \end{pmatrix} \begin{pmatrix} a_0 \\ \vdots \\ a_p \end{pmatrix} \\ &= \begin{pmatrix} \sum_{i=1}^n X^{(i)}H_0(\xi^{(i)}) \\ \vdots \\ \sum_{i=1}^n X^{(i)}H_p(\xi^{(i)}) \end{pmatrix} \end{aligned} \quad [11]$$

Both methods are illustrated in Figure 1 and in Table 1 in case of a lognormal distribution LN(0.6501, 0.2936) with a mean value of 2 and a standard deviation of 0.6.

Note that there are several methods for selecting regression points. First, they can be chosen as roots of the Hermite polynomial of order $p + 1$ (Webster *et al.*, 1996, Isukapalli, 1999). They can also be chosen randomly. This question is addressed in details in (Berveiller *et al.*, 2004b).

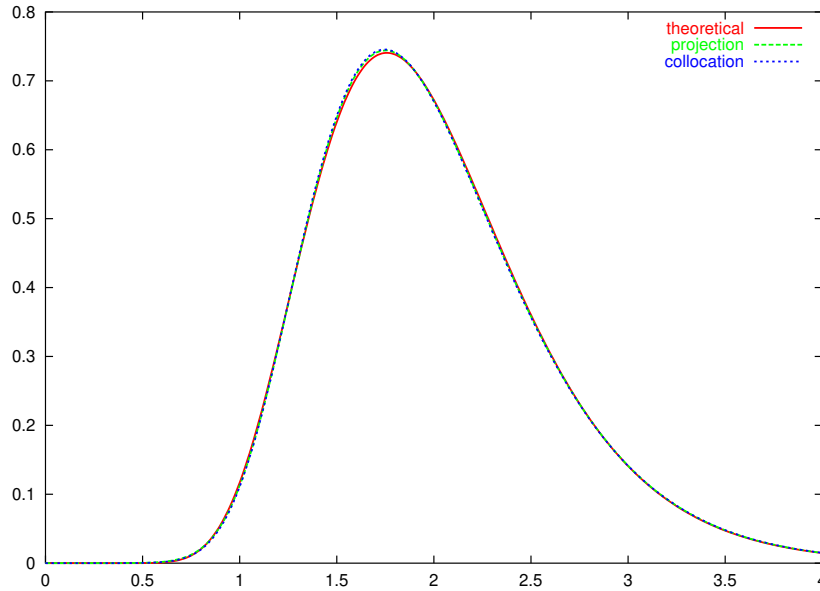


Figure 1. Theoretical and third-order approximated PDF of a lognormal distribution LN(0.6501, 0.2936)

Table 1. Coefficients of the third-order expansion of a lognormal distribution LN(0.6501, 0.2936)

Method	a_0	a_1	a_2	a_3
Projection	2.0000	0.5871	0.0862	0.0084
Regression	1.9986	0.5869	0.0872	0.0085

2.3. Error estimators

In order to qualify the accuracy of the polynomial series expansion, two error estimators are proposed. Note that the first coefficient a_0 is the mean of the random variable X under consideration. Thus it is supposed to be known. The mean square error estimator is defined as:

$$\epsilon_1 = E \left[\left(X - \tilde{X} \right)^2 \right] / \sigma^2 \tag{12}$$

where \tilde{X} is the p -th order approximation of X and σ^2 is the variance of X . From Equations [4],[9], one gets:

$$\begin{aligned} \mathrm{E} \left[(X - \tilde{X})^2 \right] &= \mathrm{E} \left[\sum_{i \geq p+1} \sum_{j \geq p+1} a_i a_j H_i(\xi) H_j(\xi) \right] \\ &= \sum_{j \geq p+1} a_j^2 \cdot j! \end{aligned} \quad [13]$$

Moreover, the variance σ^2 may be cast as:

$$\begin{aligned} \sigma^2 &= \mathrm{E} \left[(X - a_0)^2 \right] \\ &= \mathrm{E} \left[\sum_{i \geq 1} \sum_{j \geq 1} a_i a_j H_i(\xi) H_j(\xi) \right] \\ &= \sum_{j \geq 1} a_j^2 \cdot j! \end{aligned} \quad [14]$$

From the above equations, it finally comes:

$$\sigma^2 = \sum_{j=1}^p a_j^2 \cdot j! + \mathrm{E} \left[(X - \tilde{X})^2 \right] \quad [15]$$

Thus:

$$\epsilon_1 = 1 - \frac{1}{\sigma^2} \sum_{j=1}^p a_j^2 j! \quad [16]$$

The CDF error estimator is defined as:

$$\epsilon_2 = \sup_X |F_X(x) - F_{\tilde{X}}(x)| \quad [17]$$

In this expression, $F_X(x)$ is supposed to be known and $F_{\tilde{X}}(x)$ is computed from the isoprobabilistic transformation: $F_{\tilde{X}}(x) = \Phi(\xi)$. Tables 2 and 3 gather the values of both error estimators for selected random variables with prescribed mean value and standard deviation.

Table 2. Mean square error estimator ϵ_1 (%) (Equation [16])

Distribution *	Projection method			Regression method		
	order 2	order 3	order 4	order 2	order 3	order 4
Lognormal (2, 0.6)	0.00	0.00	0.00	-0.07	-3.10^{-4}	5.10^{-4}
Weibull (1, 0.36)	0.01	0.01	0.01	0.09	0.01	0.01
Gamma (2, 1.41)	0.75	0.75	0.75	0.73	0.75	0.75

* Bracketed parameters are mean value and standard deviation

It appears from these examples that 1% accuracy “in the mean region” (estimator ϵ_1) is obtained in all cases as soon as $p \geq 2$. As far as the global accuracy is concerned (estimator ϵ_2), order $p = 3$ or 4 is required to obtain a 1% accuracy.

Table 3. CDF error estimator ϵ_2 (Equation [17])

Distribution *	Projection method			Regression method		
	order 2	order 3	order 4	order 2	order 3	order 4
Lognormal (2, 0.6)	0.08	0.01	0.01	0.05	0.01	0.01
Weibull (1, 0.36)	0.06	0.02	0.01	0.04	0.01	0.01
Gamma (2, 1.41)	0.18	0.07	0.01	0.10	0.04	0.01

* Bracketed parameters are mean value and standard deviation

2.4. Functions of random variables

In the sequel, it will be required to expand functions of random variables that appear in the mechanical model (e.g. elastic coefficients as functions of the Poisson’s ratio in the Hooke law). Both methods allow to expand non linear functions of random variables. Let us denote by $h(x)$ the function under consideration. The coefficients of the expansion of $h(X)$ are obtained by projection as:

$$a_i = \frac{1}{i!} \int_{\mathbb{R}} h[F_X^{-1}(\Phi(t))] H_i(t) \varphi(t) dt \tag{18}$$

Using the regression method, the coefficients should minimize the following quantity:

$$\Delta X = \sum_{i=1}^n \left(h(X^{(i)}) - \sum_{j=0}^p a_j H_j(\xi^{(i)}) \right)^2 \tag{19}$$

where notation $(\xi^{(i)}, X^{(i)})$ has been given above. This leads to a linear system similar to Equation [11], where the right hand side is replaced by:

$$\begin{pmatrix} \sum_{i=1}^n h(X^{(i)}) H_0(\xi^{(i)}) \\ \vdots \\ \sum_{i=1}^n h(X^{(i)}) H_p(\xi^{(i)}) \end{pmatrix} \tag{20}$$

As an example, let us consider a random variable ν (e.g. Poisson’s ratio) with uniform distribution $\mathcal{U}[0.2, 0.4]$ and the non linear function $h(\nu) = 1/2(1 + \nu)$. The coefficients obtained by the two methods are listed in Table 4. It appears that the expansion coefficients are close to one another in this example.

Table 4. Coefficients of the third order expansion of the function $\frac{1}{2(1+\nu)}$ where $\nu = \mathcal{U}[0.2, 0.4]$

Method	a_0	a_1	a_2	a_3
Projection	0.3854	-0.0167	0.0004	0.0014
Regression	0.3852	-0.0167	0.0003	0.0017

2.5. Joint expansion of several independent random variables

In the sequel, various input parameters of the finite element model will be expanded onto the Hermite polynomial basis. Suppose M variables are used, each of them being expanded by means of a standard normal variable ξ_i at order n_i :

$$X^i = \sum_{k=0}^{n_i} x_k^i H_k(\xi_i) \quad i = 1, \dots, M \quad [21]$$

All these expansions are cast in a common basis called the *polynomial chaos*, which is the set of multi-dimensional Hermite polynomials (Ghanem *et al.*, 1991). Precisely, the M -th dimensional p -th order polynomial chaos is the set of multi-dimensional Hermite polynomials in $\{\xi_i\}_{i=1}^M$ whose degree does not exceed p . Let us denote by P the size of this set (its analytical expression in terms of M and p is given in Appendix I). Each polynomial is denoted by:

$$\Psi_{\alpha} = \prod_{i=1}^M H_{\alpha_i}(\xi_i), \quad \alpha_i \geq 0, \quad \sum_{i=1}^M \alpha_i \leq p \quad [22]$$

An implementation of the polynomial chaos based on symbolic calculus is proposed by (Ghanem *et al.*, 1991). In this paper we propose an original implementation based on the generation of relevant integer sequences α (see also (Sudret *et al.*, 2000)). The detail is given in Appendix I. As the uni-dimensional Hermite polynomials are contained in the polynomial chaos, Equation [21] may be rewritten as:

$$X^i = \sum_{j=0}^{P-1} \tilde{x}_j^i \Psi_j(\{\xi_k\}_{k=1}^M) \quad [23]$$

The positioning algorithm that links coefficients $\{x_k^i\}$ (Equation [21]) and $\{\tilde{x}_k^i\}$ (Equation [23]) is detailed in Appendix II.

2.6. Conclusions

In this section, two methods have been presented for the computation of a series expansion of random variables with prescribed PDF or functions thereof. Two error

estimators have been developed to qualify the accuracy of these expansions. Note the following interpretation of the methods. The projection method gives the best approximation of X at any order. The values of the coefficients do not depend on the cut-off order p . However, errors are introduced in the numerical calculation of the coefficients. On the contrary, the regression method selects the best set of coefficients for a given order p . If p is changed to $p' > p$, all the set of coefficients $\{a_0, \dots, a_{p'}\}$ will change. It is seen in Tables 2 and 3 that the error is always slightly greater in the projection method than in the regression scheme.

As a conclusion it seems that both methods are almost equivalent in terms of accuracy. The third order of expansion ($p = 3$) seems to be the best compromise between accuracy and efficiency. Correlated random variables can also be expanded onto the polynomial chaos. They are decorrelated by using a Nataf transformation (Der Kiureghian *et al.*, 1986). Then the regression method allows to jointly expand the uncorrelated random variables onto the polynomial chaos.

3. Stochastic finite element procedure (SFEP) in linear mechanics

Using classical notations (Zienkiewicz *et al.*, 2000), the finite element method for static problems in linear elasticity yields a linear system of size N_{dof} , where N_{dof} denotes the number of degrees of freedom of the structure:

$$\mathbf{K} \cdot \underline{U} = \underline{F} \tag{24}$$

In the above equation, \mathbf{K} is the global stiffness matrix, \underline{U} is the basic response quantity (e.g. vector of nodal displacements) and \underline{F} is the vector of nodal forces. In SFEP, due to the introduction of input random variables, the basic response quantity is a random vector of nodal displacements $\underline{U}(\theta)$. In this expression and in the sequel, θ denotes the random characteristics of each quantity. Each component is a random variable expanded onto the polynomial chaos:

$$\underline{U}(\theta) = \sum_{j=0}^{\infty} \underline{U}_j \Psi_j(\{\xi_k(\theta)\}_{k=1}^M) \tag{25}$$

where $\{\xi_k(\theta)\}_{k=1}^M$ denotes the set of standard normal variables appearing in the discretization of all input random variables and $\{\Psi_j, j \geq 0\}$ are multidimensional Hermite polynomials that form an orthogonal basis of $\mathcal{L}^2(\Theta, F, P)$. In the sequel, the dependency of Ψ_j in $\{\xi_k(\theta)\}_{k=1}^M$ will be omitted for the sake of clarity.

3.1. Taking into account randomness in material properties

In the deterministic case, the global stiffness matrix reads:

$$\mathbf{K} = \bigoplus_e k_e = \bigoplus_e \int_{\Omega_e} \mathbf{B}^T \cdot \mathbf{D} \cdot \mathbf{B} \, d\Omega_e \tag{26}$$

where \mathbf{B} is the matrix that relates the components of strain to the element nodal displacement, \mathbf{D} is the elasticity matrix and \bigoplus_e is the assembly procedure over all elements. When material properties are described by means of random variables, the elasticity matrix hence the global stiffness matrix become random. The latter may be expanded onto the polynomial chaos as follows:

$$\mathbf{K} = \sum_{j=0}^{\infty} \mathbf{K}_j \Psi_j \tag{27}$$

where

$$\mathbf{K}_j = \mathbb{E}[\mathbf{K}\Psi_j] = \bigoplus_e \int_{\Omega_e} \mathbf{B}^T \cdot \mathbb{E}[\mathbf{D}\Psi_j] \cdot \mathbf{B} d\Omega_e \tag{28}$$

Note that \mathbf{B} is a deterministic matrix while \mathbf{D} is random. In case of an isotropic elastic material with random independent Young’s modulus E and Poisson’s ratio ν , the latter may be written as:

$$\mathbf{D} = E(\tilde{\lambda}(\nu)\mathbf{D}_1 + 2\tilde{\mu}(\nu)\mathbf{D}_2) \tag{29}$$

where $\tilde{\lambda}(\nu)$, $\tilde{\mu}(\nu)$ are function of ν which depend on the modeling (plane strain, plane stress or three-dimensional problem) and \mathbf{D}_1 , \mathbf{D}_2 are deterministic matrices. Random Young’s modulus E is expanded as in Equation [23]. Functions of the random Poisson’s ratio $\{\tilde{\lambda}(\nu), \tilde{\mu}(\nu)\}$ (which should be mixed up with the Lamé’s coefficients of the material) may be expanded in the same way, using either the projection or the regression method:

$$\begin{aligned} E &= \sum_{i=0}^{\infty} e_i H_i(\xi_E) \\ \tilde{\lambda}(\nu) &= \sum_{j=0}^{\infty} \lambda_j H_j(\xi_\nu) \\ \tilde{\mu}(\nu) &= \sum_{j=0}^{\infty} \mu_j H_j(\xi_\nu) \end{aligned} \tag{30}$$

Note that the same standard normal variable ξ_ν is used to expand both functions $\tilde{\lambda}(\nu)$ and $\tilde{\mu}(\nu)$. By substituting for Equation [30] in Equation [29], one finally gets:

$$\begin{aligned} \mathbf{D} &= \sum_{i=0}^{\infty} \sum_{j=0}^{\infty} e_i \lambda_j H_i(\xi_E) H_j(\xi_\nu) \mathbf{D}_1 \\ &+ \sum_{i=0}^{\infty} \sum_{j=0}^{\infty} e_i \mu_j H_i(\xi_E) H_j(\xi_\nu) \mathbf{D}_2 \end{aligned} \tag{31}$$

Products $H_i(\xi_E)H_j(\xi_\nu)$ may be injected into the polynomial chaos (Section 2.5), finally yielding:

$$\mathbf{D} = \sum_{k=0}^{\infty} (\alpha_k \mathbf{D}_1 + \beta_k \mathbf{D}_2) \Psi_k \tag{32}$$

If the structure under consideration is made of several materials, the above procedure is applied using different random variables in each element group having the same material properties.

3.2. Taking into account randomness in loading

The vector of nodal forces may be written as:

$$\underline{F} = \sum_{i=1}^{N_q} q^i \underline{F}_i \quad [33]$$

where N_q is the number of load cases, $\{q^i\}_{i=1}^{N_q}$ denote random loading parameters and \underline{F}_i "load pattern" vectors corresponding to a unit value of q^i . Note that this formulation equally applies to pinpoint forces, pressure or initial stresses. Coefficients q^i can be expanded onto the polynomial chaos (see Equation [23]):

$$q^i = \sum_{j=0}^{\infty} q_j^i H_j(\xi_i) \equiv \sum_{j=0}^{\infty} \tilde{q}_j^i \Psi_j \quad [34]$$

Thus the random vector of nodal forces reads:

$$\underline{F} = \sum_{i=1}^{N_q} \sum_{j=0}^{\infty} \tilde{q}_j^i \Psi_j \underline{F}_i = \sum_{j=0}^{\infty} \tilde{\underline{F}}_j \Psi_j \quad [35]$$

3.3. Global linear system

By using Equations [25],[27],[35], the discretized stochastic equilibrium equation reads:

$$\left(\sum_{i=0}^{\infty} \mathbf{K}_i \Psi_i \right) \cdot \left(\sum_{j=0}^{\infty} \underline{U}_j \Psi_j \right) = \sum_{j=0}^{\infty} \tilde{\underline{F}}_j \Psi_j \quad [36]$$

After a truncature of the series appearing in Equation [36] at order P , the residual in the equilibrium equation is:

$$\epsilon_P = \left(\sum_{i=0}^{P-1} \mathbf{K}_i \Psi_i \right) \cdot \left(\sum_{j=0}^{P-1} \underline{U}_j \Psi_j \right) - \sum_{j=0}^{P-1} \tilde{\underline{F}}_j \Psi_j \quad [37]$$

Coefficients $\{\underline{U}_0, \dots, \underline{U}_{P-1}\}$ are computed using the Galerkin method minimizing the residual defined above, which is equivalent to requiring that this residual be orthogonal to the space spanned by $\{\Psi_j\}_{j=0}^{P-1}$ (Ghanem *et al.*, 1991):

$$\mathbb{E}[\epsilon_P \Psi_k] = 0 \quad , \quad k = \{0, \dots, P-1\} \quad [38]$$

This leads to the linear system:

$$\begin{pmatrix} \mathbf{K}_{0,0} & \cdots & \mathbf{K}_{0,P-1} \\ \mathbf{K}_{1,0} & \cdots & \mathbf{K}_{1,P-1} \\ \vdots & & \vdots \\ \mathbf{K}_{P-1,0} & \cdots & \mathbf{K}_{P-1,P-1} \end{pmatrix} \cdot \begin{pmatrix} \underline{U}_0 \\ \underline{U}_1 \\ \vdots \\ \underline{U}_{P-1} \end{pmatrix} = \begin{pmatrix} \tilde{\underline{F}}_0 \\ \tilde{\underline{F}}_1 \\ \vdots \\ \tilde{\underline{F}}_{P-1} \end{pmatrix} \quad [39]$$

denoted hereinafter by $\mathcal{K} \cdot \underline{U} = \underline{\mathcal{F}}$. In this expression, $\mathbf{K}_{j,k} = \sum_{i=0}^{P-1} \mathbf{K}_i d_{ijk}$ and $d_{ijk} = \text{E}[\Psi_i \Psi_j \Psi_k]$. Coefficients d_{ijk} may be calculated analytically (see details in Appendix I). The number of unknowns in the above linear system is $N_{dof} \times P$, where N_{dof} is the number of degrees of freedom of the mechanical model, and P is the order of expansion of each response quantity. Note that the global stiffness matrix \mathcal{K} in Equation [39] is a block matrix. The diagonal blocks represent the contribution of the mean value. When the scattering of the input parameters (*i.e.* the standard deviation of the input random variables) increases, the weight of the out-diagonal blocks increases. Figure 2 shows that the block matrix is symmetric and sparse, *i.e.* it contains a large number of zeros.

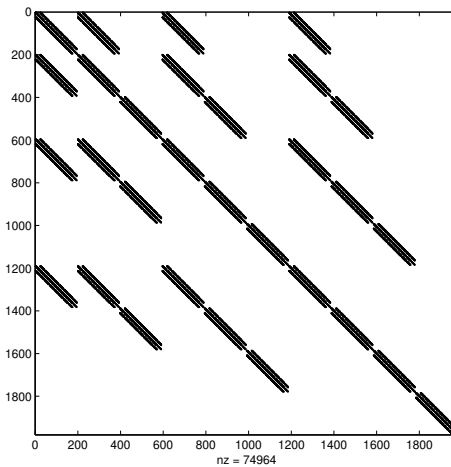


Figure 2. Representation of the global stiffness matrix \mathcal{K} (Dots are non zeros values)

The linear system Equation [39] may be solved directly (Ghanem *et al.*, 1996) by linear solvers suitable to large sparse systems (for instance, using pre-conditioned conjugate gradient techniques). A hierarchical solving scheme has also been proposed by (Ghanem, 1999a, Ghanem, 2000).

3.4. Object-oriented implementation

The implementation of the proposed stochastic finite element procedure has been made within the Matlab environment (Mathworks, 2001) in an object-oriented way. The main objects are:

- the polynomials chaos. The detail of its implementation is given in Appendix I;
- the class RANDOM_VARIABLE contains the type and parameters of each random variable, the method of approximation, the order of expansion, and the obtained expansion coefficients;
- the class MATERIAL contains all the information about material properties which may be random or deterministic. Note that a deterministic parameter may be considered as a random variable which is expanded at order 0 onto the Hermite polynomial basis. This allows a common treatment of deterministic parameters and random variables;
- the class LOADS contains all information about loading: load patterns and coefficients of load parameters expansion onto the polynomial chaos.

As presented above, the resolution of Equation [39] can be made by two ways: the direct method and the hierarchical method. Figure 3 shows an implementation scheme for the direct method.

The hierarchical method computes response coefficients by successive resolutions of systems of smaller size. Let us denote indeed by $l = \{0, \dots, Q-1, Q < P-1\}$ the *lower order* indices and $u = \{Q, \dots, P-1\}$ the *upper order* indices of the unknown vector. Equation [39] may be rewritten as:

$$\begin{pmatrix} \mathbf{K}_{l,l} & \mathbf{K}_{l,u} \\ \mathbf{K}_{u,l} & \mathbf{K}_{u,u} \end{pmatrix} \cdot \begin{pmatrix} \underline{U}_l \\ \underline{U}_u \end{pmatrix} = \begin{pmatrix} \underline{F}_l \\ \underline{F}_u \end{pmatrix} \quad [40]$$

Due to the hierarchical properties of the polynomial chaos, note that $\mathbf{K}_{l,l} \cdot \tilde{\underline{U}}_l = \underline{F}_l$ is exactly the linear system to be solved when the response is expanded at order Q . If this lower order expansion is accurate enough, it is supposed that $\tilde{\underline{U}}_l$ is a good approximation of \underline{U}_l in Equation [40]. Thus Equation [40] can be solved as follows:

$$\underline{U}_l = \tilde{\underline{U}}_l = \mathbf{K}_{l,l}^{-1} \cdot \underline{F}_l \quad [41]$$

$$\underline{U}_u = \mathbf{K}_{u,u}^{-1} \cdot (\underline{F}_u - \mathbf{K}_{u,l} \cdot \tilde{\underline{U}}_l) \quad [42]$$

$$[43]$$

In practice, order of expansion Q is related to a maximal degree $q < p$ of the multidimensional Hermite polynomials based on the M input random variables.

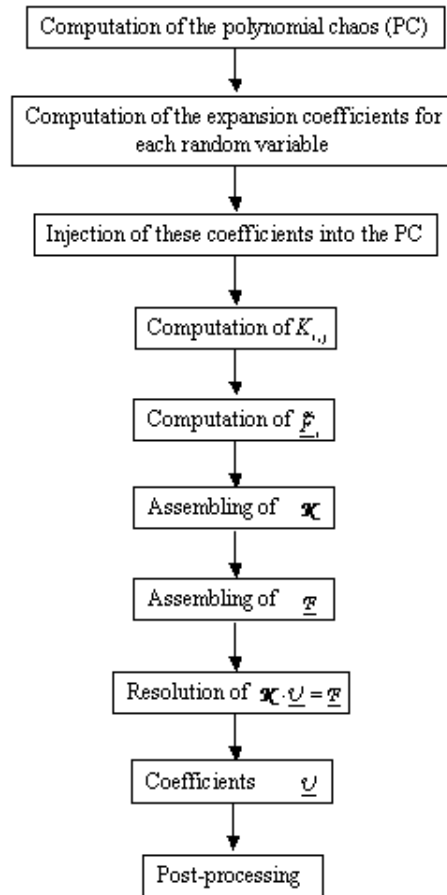


Figure 3. Implementation scheme of the direct resolution scheme

4. Post-processing of the results

Solving the linear system Equation [39] yields the expansion coefficients of the vector of nodal displacements:

$$\underline{U} = \sum_{j=0}^{P-1} \underline{U}_j \Psi_j \quad [44]$$

In this section, several results on quantities of interest are derived from the set of expansion coefficients. These results are not limited to the proposed SFEP, but apply

more generally to any stochastic finite element method based on the polynomial chaos expansion of the response.

4.1. Expansion of all response quantities

4.1.1. Strain tensor

In each element Ω_e of the finite element mesh, the strain tensor in a given point \underline{x} reads:

$$\varepsilon(\underline{x}) = \mathbf{B}(x) \cdot \underline{u}_e \quad [45]$$

where \underline{u}_e denotes the vector of nodal displacements of element e . The expansion [44] restricted to vector \underline{u}_e is:

$$\underline{u}_e = \sum_{j=0}^{P-1} \underline{u}_{e,j} \Psi_j \quad [46]$$

Thus:

$$\varepsilon(x) = \sum_{j=0}^{P-1} \varepsilon_j(x) \Psi_j \quad [47]$$

with $\varepsilon_j(x) = \mathbf{B}(x) \cdot \underline{u}_{e,j}$

4.1.2. Stress tensor

When Young's modulus E is random, whereas Poisson's ratio ν is deterministic, the elasticity matrix may be rewritten as:

$$\mathbf{D} = \left(\sum_{j=0}^{P-1} e_j \Psi_j \right) \mathbf{D}_0 \quad [48]$$

where $\{e_j\}$ are the coefficients of the expansion of E . The stress tensor $\boldsymbol{\sigma}(x)$ in a given point $x \in \Omega_e$ is:

$$\boldsymbol{\sigma}(x) = \mathbf{D} \cdot \varepsilon(x) = \sum_{i=0}^{P-1} \sum_{k=0}^{P-1} e_i \mathbf{D}_0 \cdot \varepsilon_k(x) \Psi_i \Psi_k \quad [49]$$

To simplify this expression, products $\Psi_i \Psi_k$ are injected into the polynomial chaos basis:

$$\Psi_i \Psi_k = \sum_{j=0}^{P-1} \frac{d_{ijk}}{\mathbb{E}[\Psi_j^2]} \Psi_j \quad [50]$$

One finally gets:

$$\begin{aligned} \boldsymbol{\sigma}(x) &= \sum_{j=0}^{P-1} \boldsymbol{\sigma}_j \Psi_j \\ \text{with } \boldsymbol{\sigma}_j(x) &= \sum_{i=0}^{P-1} \sum_{k=0}^{P-1} d_{ijk} e_i \mathbf{D}_0 \cdot \boldsymbol{\varepsilon}_k(x) \end{aligned} \quad [51]$$

When both Young's modulus E and Poisson's ratio ν are random, the elasticity matrix is:

$$\mathbf{D} = \sum_{i=0}^{P-1} (\alpha_i \mathbf{D}_1 + \beta_i \mathbf{D}_2) \Psi_i \quad [52]$$

where coefficients (α_i, β_i) have been given in section 3.1. Then the stress tensor becomes:

$$\begin{aligned} \boldsymbol{\sigma}(x) &= \sum_{j=0}^{P-1} \boldsymbol{\sigma}_j \Psi_j \\ \text{with } \boldsymbol{\sigma}_j(x) &= \sum_{i=0}^{P-1} \sum_{k=0}^{P-1} d_{ijk} (\alpha_i \mathbf{D}_1 + \beta_i \mathbf{D}_2) \cdot \boldsymbol{\varepsilon}_k(x) \end{aligned} \quad [53]$$

As a conclusion, it appears that the mechanical response of the system \underline{S} (*i.e.* the set of all nodal displacements, nodal strain or stress components) may be written as:

$$\underline{S} = \sum_{j=0}^{P-1} \underline{S}_j \Psi_j. \quad [54]$$

4.2. Moment analysis

From Equation [54], the statistical moments of any response quantity can be easily computed. The mean of the response quantity S (nodal displacement, strain or stress component) is given by:

$$E[S] = s_0 \quad [55]$$

The variance of S is:

$$\text{Var}[S] = \sigma_S^2 = \sum_{i=1}^{P-1} E[\Psi_i^2] s_i^2 \quad [56]$$

The skewness and the kurtosis coefficients of S are:

$$\delta_S = \frac{1}{\sigma_S^3} \sum_{i=1}^{P-1} \sum_{j=1}^{P-1} \sum_{k=1}^{P-1} d_{ijk} s_i s_j s_k \quad d_{ijk} = E[\Psi_i \Psi_j \Psi_k] \quad [57]$$

$$\kappa_S = \frac{1}{\sigma_S^4} \sum_{i=1}^{P-1} \sum_{j=1}^{P-1} \sum_{k=1}^{P-1} \sum_{l=1}^{P-1} d_{ijkl} s_i s_j s_k s_l \quad d_{ijkl} = E[\Psi_i \Psi_j \Psi_k \Psi_l] \quad [58]$$

Note that coefficients (d_{ijk}, d_{ijkl}) are known analytically (See Appendix I).

4.3. Finite element reliability analysis

In reliability analysis (Ditlevsen *et al.*, 1996), the failure criterion of a structure is defined in terms of a limit state function $g(\underline{X}, \underline{S}(\underline{X}))$ which may depend both on basic random variables \underline{X} and response quantities $\underline{S}(\underline{X})$. The domain $\{g(\underline{X}, \underline{S}(\underline{X})) > 0\}$ defines the safe state and $\{g(\underline{X}, \underline{S}(\underline{X})) \leq 0\}$ defines the failure state. Using this notation, the aim of reliability analysis is to compute the probability of the failure event:

$$\begin{aligned} P_f &= \text{Prob}[g(\underline{X}, S(\underline{X})) \leq 0] \\ &= \int_{g(\underline{X}, S(\underline{X})) \leq 0} f_{\underline{X}}(\underline{x}) d\underline{x} \end{aligned} \quad [59]$$

where $f_{\underline{X}}(\underline{x})$ is the joint probability density function of the random variables \underline{X} . The computation of this integral is not possible directly because the failure domain depends implicitly on $\underline{S}(\underline{X})$, which is computed using a finite element code.

The First Order Reliability Method (FORM) has proven efficiency together with finite element analysis for approximating the probability of failure (Der Kiureghian *et al.*, 1988, Lemaire, 1998). However, this approach, which is based on an iterative optimization algorithm that provides the design point (most probable failure point in the standard normal space) may be computationally expensive. It requires indeed successive deterministic finite element runs until convergence of the algorithm is obtained. By the way, any parametric study requires rerun the full coupled model, without being able to reuse the previous finite element calculations.

The SFEP developed in the above section offers an attractive alternative for finite element reliability analysis. It has been shown indeed that any response quantity can be cast as a series expansion, whose coefficients results from Equations [44],[47],[53]. Thus any limit state function may be approximated as follows, once a stochastic finite element analysis has been carried out:

$$g(\underline{X}, S(\underline{X})) \cong g\left(\{\xi_k\}_{k=1}^M, \sum_{j=0}^{P-1} \underline{S}_j \Psi_j(\{\xi_k\}_{k=1}^M)\right) \quad [60]$$

Then the reliability problem, which is already formulated in the standard normal space by construction, may be solved by any available method including Monte-Carlo Simulation, FORM/SORM, Importance Sampling, etc. (Ditlevsen *et al.*, 1996).

4.4. Representation of the response PDF

Three methods for representing the probability density function of response quantities are presented in this section.

4.4.1. Histograms

The first method is the classical Monte-Carlo simulation, which generates an histogram from n samples. The number of bins n_{bin} of the histogram can be computed using the Stuge's rule:

$$n_{bin} = 1 + \log_2(n) \quad [61]$$

This requires only simulating samples of the standard normal vector $\underline{\xi} = \{\xi_1, \dots, \xi_M\}$. Note that the simulation is inexpensive in our case since each response quantity is a polynomial function of $\underline{\xi}$.

4.4.2. Averaged shifted histograms

The idea behind this method is to generate several histograms, which have the same bin width Δx but different origins, and to average them in order to obtain a smoother histogram (Yu, 2003). Let us consider m histograms $\{h_1(x), \dots, h_m(x)\}$, whose origin are respectively:

$$x'_0 = x_0, x_0 + \frac{\Delta x}{m}, x_0 + \frac{2\Delta x}{m}, \dots, x_0 + \frac{(m-1)\Delta x}{m} \quad [62]$$

The mean histogram is then obtained by:

$$h_{moy} = \frac{1}{m} \sum_{i=1}^m h_i(x) \quad [63]$$

4.4.3. Parametric FORM analysis

Let us consider a component S of the random response vector \underline{S} whose PDF $f_S(x)$ is looked after. The CDF $F_S(x)$ may be considered as the solution of a reliability problem. Indeed:

$$\begin{aligned} F_S(x) &= P(S \leq x) \\ &= P\left(\sum_{j=0}^{P-1} S_j \Psi_j(\{\xi_k\}_{k=1}^M) - x \leq 0\right) \\ &= P(g_S(\underline{\xi}, x) \leq 0) \end{aligned} \quad [64]$$

where

$$g_S(\underline{\xi}, x) = \sum_{j=0}^{P-1} S_j \Psi_j(\{\xi_k\}_{k=1}^M) - x \quad [65]$$

Suppose that $\beta(x)$ is the reliability index associated with the above reliability problem, and $P_f(x) = \Phi(-\beta(x))$ is the corresponding FORM approximation. Straightforward algebra yields:

$$\begin{aligned} f_S(x) &= \frac{dF_S(x)}{dx} \\ &= \frac{d\Phi(-\beta(x))}{dx} \\ &= -\varphi(\beta(x)) \cdot \frac{d\beta(x)}{dx} \end{aligned} \quad [66]$$

The quantity $\frac{d\beta(x)}{dx}$ may now be considered as the sensitivity of $\beta(x)$ with respect to parameter x . Analytical results for this kind of problem have been given in (Ditlevsen *et al.*, 1996):

$$\frac{d\beta(x)}{dx} = \frac{1}{\left\| \nabla_{\underline{\xi}} g_S(\underline{\xi}, x) \right\|_{\underline{\xi}=\underline{\xi}^*}} \frac{\partial g_S(\underline{\xi}, x)}{\partial x} \quad [67]$$

where the gradient appearing in the denominator is evaluated at the design point $\underline{\xi} = \underline{\xi}^*$ (most likely failure point in the standard normal space). Due to Equation [65], $\frac{\partial g_S(\underline{\xi}, x)}{\partial x} = -1$. Thus:

$$f_S(x) = \frac{\varphi(\beta(x))}{\left\| \nabla_{\underline{\xi}} g_S(\underline{\xi}, x) \right\|_{\underline{\xi}=\underline{\xi}^*}} \quad [68]$$

As a conclusion, the PDF of any response quantity S may be obtained by successive FORM analysis with different values of threshold x , using Equation [68]. Note that this method provides a smooth representation of $f_S(x)$, in contrary to histograms. The FORM analysis are inexpensive since the underlying limit state function is analytical (Equation [64]) and already formulated in the standard normal space.

5. Application examples in geotechnical engineering

5.1. Example #1: homogeneous soil layer

5.1.1. Deterministic problem statement

Let us consider an elastic soil mass made of an isotropic linear elastic material lying on a rigid substratum. A foundation on this soil mass is modeled as a uniform pressure load P applied over a length $2B$ of the free surface (Figure 4). Due to the symmetry, half of the structure is modeled by finite element. The mesh of half of the foundation comprises 99 nodes and 80 4-node elements which allows a 1%-accurate evaluation of the maximal settlement compared to a reference solution (Figure 5).

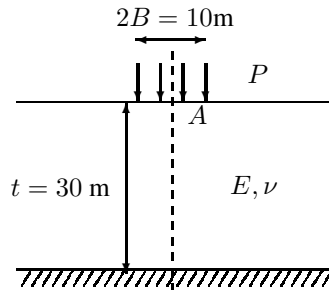


Figure 4. Homogeneous soil layer: scheme of the fondation

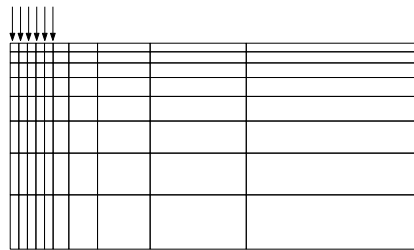


Figure 5. Mesh of the foundation

The model parameters are listed in Table 5. As the soil mass has an elastic behavior, the maximal settlement is given by:

$$U^{i_0} = \chi \frac{P}{E} \quad [69]$$

The numerical value of χ is 13.575 m for the mesh under consideration, corresponding to a maximal settlement $U_{max}=0.0543$ m (the “exact” solution obtained with a refined mesh is $\chi = 13.744$ m).

Table 5. Homogeneous soil layer: parameters of the foundation

Parameter	Notation	Mean Value
Young’s Modulus	E	50 MPa
Poisson’s Ratio	ν	0.3
Load	P	0.2 MPa
Width of the foundation	$2B$	10 m
Mesh size	L	60 m
Soil thickness	t	30 m

5.1.2. Stochastic problem

In this first example, we consider that there are only two random variables: the Young's modulus E and the applied load P . The Young's modulus is represented by a lognormal random variable with a mean value $\mu_E = 50$ MPa and a coefficient of variation of 20%. The load is represented by a lognormal variable with mean $\mu_P = 0.2$ MPa and a coefficient of variation of 20%. As P and E are lognormal random variables, U^{i_0} is also a lognormal random variable with parameters $\lambda_U = \ln(\chi) + \lambda_P - \lambda_E = -2.9022$ and $\zeta_U = \sqrt{\zeta_P^2 + \zeta_E^2} = 0.2801$.

Table 6. Homogeneous soil layer: coefficients of the polynomial chaos expansion of U^{i_0}

$p = 2$	Direct		$p = 3(2)$	Hierarchical	
	$p = 3$	$p = 4$		$p = 4(2)$	$p = 4(3)$
-5.64E-02	-5.64E-02	-5.64E-02	-5.64E-02	-5.64E-02	-5.64E-02
-1.12E-02	-1.12E-02	-1.12E-02	-1.12E-02	-1.12E-02	-1.12E-02
1.11E-02	1.12E-02	1.12E-02	1.11E-02	1.11E-02	1.12E-02
-5.32E-04	-5.53E-04	-5.53E-04	-5.32E-04	-5.32E-04	-5.53E-04
2.13E-03	2.21E-03	2.21E-03	2.13E-03	2.13E-03	2.21E-03
-1.02E-03	-1.11E-03	-1.11E-03	-1.02E-03	-1.02E-03	-1.11E-03
	-1.17E-05	-1.22E-05	-1.17E-05	-1.17E-05	-1.17E-05
	1.05E-04	1.09E-04	-4.06E-04	-4.06E-04	1.05E-04
	-2.11E-04	-2.19E-04	-1.16E-05	-1.16E-05	-2.11E-04
	7.34E-05	7.28E-05	2.44E-05	2.45E-05	7.34E-05
		-1.45E-07		-1.45E-07	-1.45E-07
		2.32E-06		7.73E-05	-2.01E-05
		-1.04E-05		-3.65E-05	-7.29E-07
		1.39E-05		7.13E-07	-6.74E-06
		-3.32E-06		1.44E-06	1.46E-06

Table 6 collects the expansion coefficients of the settlement U^{i_0} obtained by SFEP at different orders with the two methods of resolution (direct and hierarchical). Note that p is the degree of the polynomial chaos expansion. The notation $p = 3(2)$ means "hierarchical resolution at order 3 with a pre-resolution at the order 2". It is observed that the values of the lower order (six first) coefficients computed at order 3 or 4 are close to the values computed at order 2. This is a justification of the use of the hierarchical approach.

5.1.3. Statistical analysis

The statistical moments obtained from Equations [55]-[58] after SFEP analysis are collected in Table 7. Since U^{i_0} is a lognormal random variable whose parameters have been computed above, exact values of these moments are also available (Table 7, column #2).

Table 7. *Homogeneous soil layer: moments of the maximal settlement U^{i0}*

	Theoretical		Direct	
	values	$p = 2$	$p = 3$	$p = 4$
mean/ U_{max}	1.0286	1.0273	1.0278	1.0278
coeff. var.	0.2857	0.2837	0.2846	0.2846
skewness	-0.8803	-0.6831	-0.7573	-0.7599
kurtosis	4.4088	3.6366	4.0050	4.0373
		Hierarchical		
		$p = 3(2)$	$p = 4(2)$	$p = 4(3)$
mean/ U_{max}		1.0278	1.0278	1.0280
coeff. var.		0.2838	0.2838	0.2846
skewness		-0.6517	-0.6493	-0.7565
kurtosis		3.4233	3.4713	3.9884

One can note that for the mean and the coefficient of variation, all solving schemes provide accurate results (about 1% discrepancy compared to the exact values). The estimation of the skewness and kurtosis coefficients becomes accurate with increasing order of the polynomial chaos. The direct resolution method gives better results than the hierarchical method but the difference is often insignificant.

Table 8. *Homogeneous soil layer: computer processing time (s)*

Deterministic	Direct			Hierarchical		
	$p = 2$	$p = 3$	$p = 4$	$p = 3(2)$	$p = 4(2)$	$p = 4(3)$
0.82	3.74	8.43	53.76	5.9	7.7	10.88

Computer processing time (CPT) associated to each scheme is reported in Table 8 (the simulations were run on Pentium 4 PC at 1.7 GHz, the results are given in seconds). It is observed that the CPT increases fast when the direct approach is used. The hierarchical resolution allows to decrease the CPT by a factor of 5 or more. This shows the relevance of such schemes, since the results obtained by those are quite close to the results obtained by the direct approach, as explained above.

5.1.4. Reliability analysis

The aim of this section is to compute the reliability index associated with the maximum settlement of a foundation. The limit state-function is:

$$g(\mathbf{U}) = u_S - U^{i0} \quad [70]$$

where u_S denotes the threshold. Since U^{i0} is lognormal, it can be written as (ξ denotes a standard normal random variable):

$$U^{i0} = \exp[\lambda_U + \zeta_U \xi] \quad [71]$$

Thus the limit state function is equivalent to:

$$g_2(\xi) = \ln(u_S) - (\lambda_U + \zeta_U \xi) \tag{72}$$

The associated reliability index straightforwardly reads:

$$\beta = \frac{\ln(u_S) - \lambda_U}{\zeta_U} = \frac{\ln(u_S) - \ln(\chi) - \lambda_P + \lambda_E}{\sqrt{\zeta_P^2 + \zeta_E^2}} \tag{73}$$

and the exact value of the probability of failure is:

$$P_f = \Phi(-\beta) \tag{74}$$

On the other hand, by using the SFEP solution for having the polynomial chaos expansion of U^{i_0} , Equation [70] becomes:

$$g(U) = u_S - \sum_{j=0}^{P-1} U_j^{i_0} \Psi_j(\xi_E, \xi_P) \tag{75}$$

An efficient way of accurately compute the probability of failure associated with such a limit state function is the so-called *importance sampling* technique. First FORM analysis is applied in order to find the design point. Then Monte Carlo simulation is applied by concentrating samples around the design point. In the present study, importance sampling is applied using 1,000 simulations. The estimated probability of failure $P_{f,IS}$ is obtained with a coefficient of variation of less than 5%. The equivalent reliability index $\beta_{IS} = -\Phi^{-1}(P_{f,IS})$ obtained by the analytical solution and various approximations using SFEP are given in Table 9.

Table 9. Homogeneous soil layer: reliability index β_{IS}

Threshold (m)	Theoretical Eq. [73]	Stochastic Finite Element Procedure (Eq. [75] + FORM)					
		Direct			Hierarchical		
		$p = 2$	$p = 3$	$p = 4$	$p = 3(2)$	$p = 4(2)$	$p = 4(3)$
0.07	0.8626	0.8704	0.8841	0.8848	0.8650	0.8684	0.8828
0.08	1.3394	1.3724	1.3752	1.3769	1.3731	1.3808	1.3726
0.09	1.7599	1.8331	1.8148	1.8162	1.8478	1.8561	1.8119
0.10	2.1361	2.2612	2.2137	2.2132	2.2971	2.3000	2.2116
0.12	2.7871	3.0421	2.9185	2.9090	3.1389	3.1075	2.9217
0.15	3.5838	4.0768	3.8099	3.7766	4.2973	4.1494	3.8292
0.17	4.0307	4.7002	4.3257	4.2713	5.0146	4.7484	4.3606
0.20	4.6110	5.5610	5.0149	4.9231	6.0202	5.5272	5.0787

The theoretical reliability index is computed using Equation [73]. As expected, the accuracy in the computed reliability indices increases with the order p of the response expansion in the direct solving scheme. The gain between orders 2 and 3 is always greater than the gain between orders 3 and 4. Order $p = 3$ thus appears to be a

good compromise between accuracy and efficiency. It allows to get accurate results (e.g. within 5-10% discrepancy compared to the exact solution) in a broad range of reliability indices $\beta = [0.8 - 4.6]$.

By comparing the hierarchical vs. the direct results (e.g. $p = 3(2)$ vs. $p = 2$), one can see that the hierarchical step does not degrade much the results in this case, whereas the computation time has been divided by 2-5 compared to the direct resolution effort (see Table 8).

5.1.5. Probability density function of the maximal displacement

The PDF of the maximal displacement is plotted in Figure 6 with the method presented in Section 4.4.3. The reference PDF is plotted from the analytical expression of the PDF of a lognormal random variable. PDFs that are closest to the reference PDF are those computed by SFEP at an order $p \geq 3$.

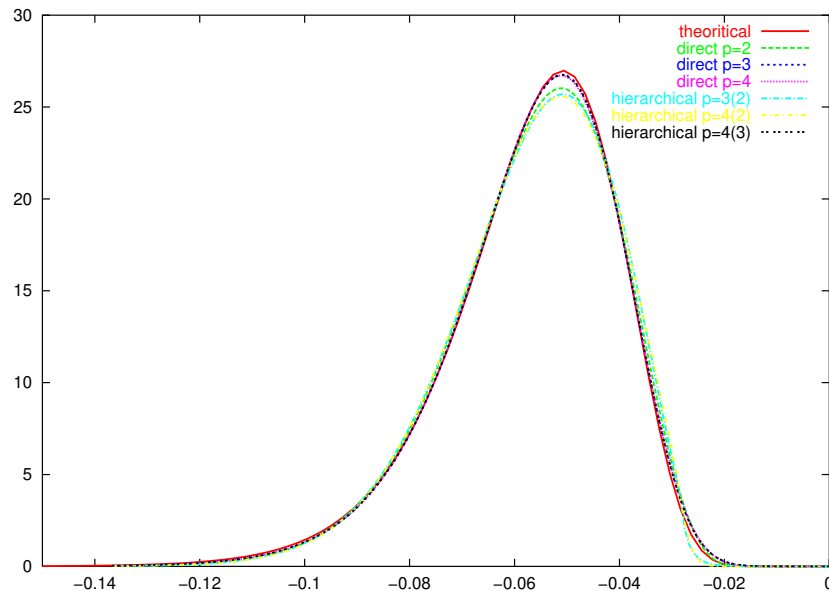


Figure 6. Homogeneous soil layer: PDF of the maximal settlement

5.2. Example #2: two-layer soil mass submitted to two loads (Sudret et al., 2004)

5.2.1. Deterministic problem statement

Let us consider an elastic soil mass made of two layers of different isotropic linear elastic materials lying on a rigid substratum (Figure 7). A foundation on this soil mass is modeled by two uniform pressures P_1 and P_2 applied over a length $2B$ of the free surface (Figure 5).

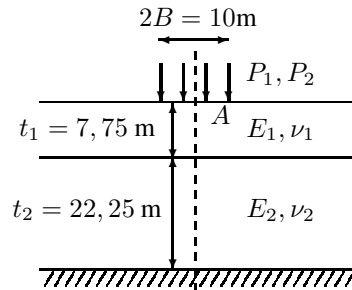


Figure 7. Two-layer soil layer mass: scheme of the foundation

Due to the symmetry, half of the structure is modeled by finite element. The mesh is the same as in section 5.1 (Figure 5). The model parameters are listed in Table 10.

Table 10. Two-layer soil layer mass: parameters of the foundation

Parameter	Notation	Mean
Upper layer Young's Modulus	E_1	50 MPa
Lower layer Young's Modulus	E_2	70 MPa
Upper layer Poisson's Ratio	ν_1	0.3
Lower layer Poisson's Ratio	ν_2	0.3
Load #1	P_1	0.2 MPa
Load #2	P_2	0.2 MPa
Width of the foundation	$2B$	10 m
Mesh size	L	60 m
Upper layer soil thickness	t_1	7.75 m
Lower layer soil thickness	t_2	22.25 m

5.2.2. Stochastic problem

The upper (resp. lower) layer Young's modulus is represented by a lognormal random variable with a mean value $\mu_{E_1} = 50$ MPa (resp. $\mu_{E_2} = 70$ MPa) and a coefficient of variation $CoV_{E_1} = 20\%$. Both layers' Poisson's ratio are represented by uniform random variables defined on $[0.28, 0.32]$. The applied loads are represented by a Weibull random variable (mean value $\mu_{P_1} = 0.2$ MPa, coefficient of variation $CoV_{P_1} = 20\%$) and a lognormal random variable (mean value $\mu_{P_2} = 0.2$ MPa and coefficient of variation of $CoV_{P_2} = 20\%$) respectively. All six random variables are supposed independent.

In this example, no analytical results are available. Reference results presented in the sequel are obtained by coupling the probabilistic code PROBAN (Det Norske Veritas, 2000) and the finite element code Code_Aster [<http://www.code-aster.org>].

5.2.3. Statistical analysis

In this section, the statistical moments of the maximal settlement of the foundation are computed. The reference solution is obtained using Monte Carlo simulation with 10,000 samples. Using SFEP, the direct solving scheme at order $p = 2$ (resp. $p = 3$) is considered. Since the problem involves 6 random variables, the number of response coefficients for each degree of freedom is 28 (resp. 84). The hierarchical scheme $p = 3(2)$ is also considered. Table 11 gathers the results.

Table 11. Two-layer soil layer mass: moments of the maximal settlement

	Monte Carlo Simulation*	direct $p = 2$	$p = 3$	hierarchical $p = 3(2)$
mean/ U_{max}	1.04	1.04	1.04	1.04
Coeff. Var.	0.23	0.22	0.23	0.22
skewness	-0.45	-0.42	-0.45	-0.42
kurtosis	3.39	3.28	3.39	3.28

* 10,000 samples

Here again it is observed that $p = 2$ is sufficient to get accurately the mean and standard deviation of the response. The order $p = 3$ is required to obtain also an accurate estimation of the skewness and kurtosis coefficients, either by direct or hierarchical analysis.

Table 12. Two-layer soil layer mass: computer processing time (s)

	Deterministic $p = 0$	SFEP Direct $p = 2$	$p = 3$	SFEP Hierarchical $p = 3(2)$
Number of coefficients	1	28	84	84
CPT	1	83	2003	174

Table 12 gathers the CPT for this second example (the time unit corresponds to a deterministic finite element run). Due to the number of variables, the computational effort is 25 times greater for a third order analysis compared to a second order analysis. Note that this factor is reduced to 2 when the hierarchical approach is selected. This makes the latter attractive as a compromise between accuracy and efficiency.

5.2.4. Reliability analysis

The limit state function under consideration is identical to that used in the first example, see Equation [70]. The reliability index is computed by various methods for different admissible maximal settlement and compared. The results are gathered in Table 13. Note that more accurate results could be obtained by importance sampling

after SFEP. However, these results would not be directly comparable to the FORM results obtained by the coupling PROBAN/Code_Aster.

Table 13. *Two-layer soil layer mass: reliability index β .*

Threshold (m)	β_{ref}	β_{SFEP}		
	FORM	$p = 2$	$p = 3$	$p = 3(2)$
0.10	0.3353	0.3195	0.3286	0.3175
0.12	1.1683	1.1553	1.1662	1.1434
0.15	2.2471	2.2634	2.2496	2.2390
0.20	3.7040	3.8483	3.7334	3.8061
0.25	4.8633	5.2171	4.9510	5.1560
0.30	5.8171	6.4388	5.9911	6.3546

The reference results are obtained by FORM analysis using a coupling between PROBAN and the finite element code Code_Aster.

The other results are obtained by applying FORM after SFEP analysis. The conclusions drawn in the first example are still valid: the accuracy of the approach is satisfactory (less than 3% discrepancy compared to the reference) for a large range of reliability indices $\beta = [0.3, 5.8]$, and even better than in the first example. In the present case, the hierarchical scheme $p = 3(2)$ allows to improve results compared to the scheme $p = 2$.

Note that only the FORM reliability indices are presented in Table 13 in order to compare with the reference FORM analysis. It is of course possible to post-process at low cost the SFEP results using crude Monte Carlo simulation or accelerated methods such as importance sampling.

5.3. Example #3: fragility curve of the foundation (Sudret et al., 2003)

Let us consider an elastic soil mass made of two layers of different isotropic linear elastic materials lying on a rigid substratum (Figure 7). A foundation on this soil mass is modeled as a uniform pressure λP_0 applied over a length $2B$ of the free surface (where P_0 denotes the unit pressure). There are four random variables, namely the Young's modulus and Poisson's ratio of each layer. The model parameters are listed in Table 14.

The reliability of the foundation with respect to the maximum admissible settlement u_S is investigated as a function of the applied pressure denoted hereinafter by λ . The result is the so-called *fragility curve*. Hence the parametric limit state function:

$$g(\underline{X}, \lambda) = u_S - \lambda U^{i_0}(E_1, \nu_1, E_2, \nu_2) \quad [76]$$

Table 14. *Two-layer soil mass - parameter study: parameters of the foundation*

Parameter	Notation	Type	Mean	Coef. of Var.
Upper layer Young's Modulus	E_1	Lognormal	50 MPa	20%
Lower layer Young's Modulus	E_2	Lognormal	70 MPa	20%
Upper layer Poisson's Ratio	ν_1	Beta [0, 0.5]	0.3	20%
Lower layer Poisson's Ratio	ν_2	Beta [0, 0.5]	0.3	20%
Width	$2B$	Deterministic	10 m	-
Mesh width	L	Deterministic	60 m	-
Upper layer soil thickness	t_1	Deterministic	7.75 m	-
Lower layer soil thickness	t_2	Deterministic	22.25 m	-
Threshold	u_S	Deterministic	0.1 m	-

where $U^{i_0}(E_1, \nu_1, E_2, \nu_2)$ is the maximal displacement obtained for a unit pressure (*i.e.* $\lambda = 1$). The reliability index is computed by FORM for different values of λ using the two strategies, namely:

– a direct coupling between the finite element code Code_Aster and the probabilistic code PROBAN using the “parametric study” feature;

– a *single* SFEP analysis leading to a polynomial chaos approximation of $U^{i_0}(E_1, \nu_1, E_2, \nu_2)$ followed by a parametric FORM reliability analysis. These tools are implemented in a Matlab package.

Table 15. *Two-layer soil mass - parameter study: reliability index vs. load parameter λ*

λ (MPa)	Direct Coupling	SFEP		
		$p = 2$	$p = 3$	$p = 3(2)$
0.100	9.4605	12.0038	10.7559	10.7350
0.150	6.9900	7.9454	7.6122	7.6175
0.200	5.1135	5.4536	5.4004	5.4047
0.250	3.6212	3.7013	3.7412	3.7228
0.300	2.3963	2.3674	2.4322	2.4024
0.350	1.3637	1.2971	1.3622	1.3377
0.400	0.4732	0.4054	0.4612	0.4536
0.450	-0.3084	-0.3589	-0.3183	-0.3037
0.500	-1.0022	-1.0285	-1.0091	-0.9723
0.550	-1.6268	-1.6257	-1.6351	-1.5799
0.600	-2.1942	-2.2657	-2.2133	-2.1463

Results are reported in Table 15. Column #2 corresponds to the reference solution (direct coupling between Code_Aster and PROBAN), columns #3-5 correspond to different strategies of resolution in the SFEP analysis, namely a complete resolution

at order 2 or 3 and a hierarchical resolution at order 3 with pre-resolution at order 2. The evolution of the reliability index (resp. the probability of failure) is plotted in Figures 8-9 as a function of the load parameter.

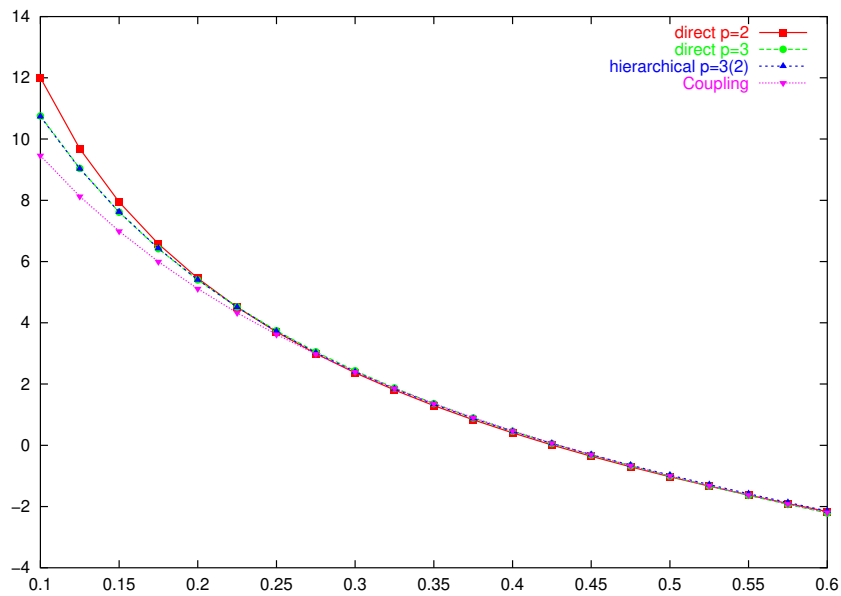


Figure 8. Two-layer soil mass - parameter study: reliability index vs. load parameter

As in the previous sections, a good agreement is observed for a large range of reliability indices, namely $\beta = [-2, 5]$. In this example, the results obtained with a second order polynomial chaos expansion are rather satisfactory (less than 10% discrepancy in β).

Table 16. Two-layer soil mass - parameter study: total computer processing time required by the direct coupling and by SFEP at various orders

	Direct	SFEP			
	Coupling	$p = 0$	$p = 2$	$p = 3$	$p = 3(2)$
CPT	1280	1	56	1291	105

Table 16 reports the computer processing time for the complete parametric study in each case, where the unit time corresponds to one single deterministic analysis (*i.e.* $p = 0$ in the SFEP context). It appears that the direct coupling is about as computationally expensive as SFEP at third order. However the same accuracy is obtained for SFEP ($p = 3(2)$) hierarchical solution at about *one tenth* of the cost. As a conclusion, the hierarchical solution $p = 3(2)$ offers a good compromise between accuracy and efficiency in this third example.

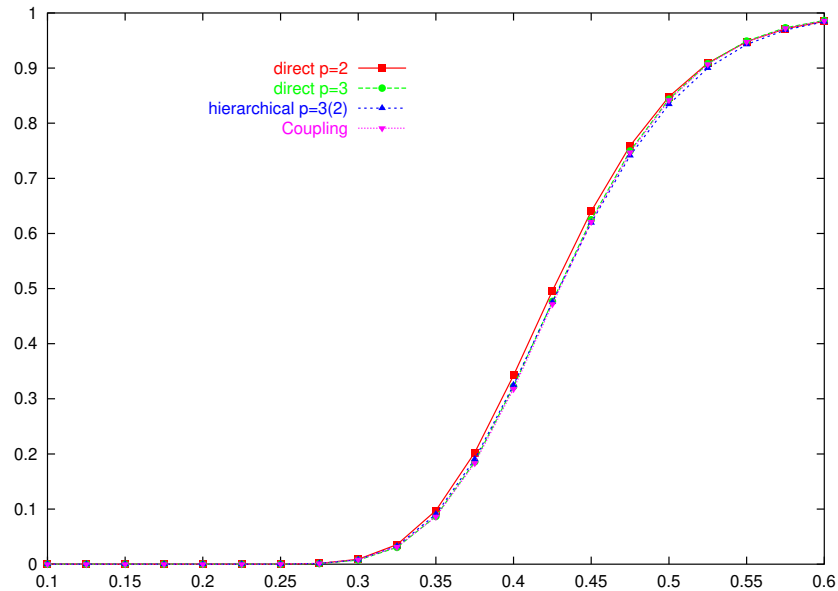


Figure 9. *Two-layer soil mass - parameter study: probability of failure vs. load parameter*

6. Conclusion

An original stochastic finite element procedure in the tradition of Ghanem's work has been proposed. The method is based on a) the representation of input random variables in terms of Hermite series expansions of standard normal variates b) the polynomial chaos expansion of the response by means of multi-dimensional Hermite polynomials. The method allows to include any number of random variables of any type for modeling the uncertainties in material parameters (Young's modulus, Poisson's ratio) and loading.

An original implementation of the polynomial chaos and related tools is proposed. This should allow new researchers to take over the technique more easily.

A great amount of work has been devoted to clarify the post-processing of the response coefficients obtained by SFEP. The expansion of derived quantities such as strain or stresses is presented. The post-processing of SFEP for moment analysis has been detailed: analytical expressions of the first four moments of response quantities are given. The post-processing of SFEP for reliability analysis has been presented. Finally an efficient method based on sensitivity FORM analysis has been given for plotting smooth PDFs of response quantities.

The proposed SFEP is applied to three geotechnical problems related to the settlement of a foundation. The first truly simple problem (which involves only two random

variables) is presented as a validation example since an analytical solution of the response moments (resp. the probability of failure or equivalently, the reliability index) is available. The second problem is more general and involves six random variables. The third problem deals with the *fragility curve* of the foundation, *i.e.* the evaluation of the probability of failure by exceeding an admissible settlement as a function of the applied loading.

Through these three examples, several numerical schemes have been tested, namely a direct solver at different orders and a so-called hierarchical solver. It follows from this investigation that the second-order polynomial chaos expansion of the response should be used when only mean and standard deviation of the response are sought (this is the common practice in the literature). However, when higher order moments are sought, or when reliability analysis (which involves the tails of the variables' PDFs) is concerned, the third-order expansion has to be used. A quicker computation of the third-order response coefficients by a hierarchical solver (called $p = 3(2)$ in the above section) appears a good compromise between accuracy and efficiency. The SFEP post-processing for parametric reliability study (fragility curve) is an example in which the proposed method is faster than usual techniques (e.g. repeated FORM analysis).

Finally, it is believed that the systematic link between polynomial chaos expansions (PCEM) and random field representations, which is commonly implicit in many papers related to stochastic finite element analysis should be broken, as demonstrated in the paper. This may help these PCEM come out the circle of university laboratories and become mature for true industrial applications which do not always need to include spatial variability. Note that the use of random fields together with random variables is straightforward using the presented framework provided the field has been previously discretized, e.g. using the Karhunen-Loève expansion (Ghanem *et al.*, 1991), the Orthogonal Series Expansion (OSE) method (Zhang *et al.*, 1994) or the Expansion Optimal Linear Estimation (EOLE) method (Li *et al.*, 1993).

Again within the framework of polynomial chaos expansion of the response, alternative methods for computing the response coefficients may be considered in the future: the *non intrusive method* used by (Ghiocel and Ghanem, 2002, Choi *et al.*, 2004a;2004b) or the *regression method* (Berveiller *et al.*, 2006). These methods have been investigated and compared to the present SFEP by (Berveiller *et al.*, 2004a; 2004b). A summary of these investigations can be found in (Sudret, 2005). These approaches appear already attractive, since they transform the stochastic finite element problem into a succession of deterministic analysis, which can of course be carried out by any commercial finite element code without intrusive implementation. Moreover, the assembling and inversion of a large linear system such as Equation [39] is avoided. This is of crucial importance for being able to deal with a larger number of random variables. Finally, non linear stochastic finite element problems can be solved without additional trouble using these non intrusive approach, provided the finite element code at hand allows to solve the related deterministic problem. An application example in non linear fracture mechanics can be found in (Berveiller *et al.*, 2005).

7. References

- Anders M., Hori M., "Stochastic finite element method for elasto-plastic body", *Int. J. Num. Meth. Eng.*, vol. 46, n° 11, 1999, p. 1897-1916.
- Anders M., Hori M., "Three-dimensional stochastic finite element method for elasto-plastic body", *Int. J. Numer. Met. Engng.*, vol. 51, 2001, p. 449-478.
- Babuska I., Chatzipantelidis P., "On solving elliptic stochastic partial differential equations", *Comp. Meth. Appl. Mech. Eng.*, vol. 191, n° 37-38, 2002, p. 4093-4122.
- Berveiller M., Sudret B., Lemaire M., "Comparison of methods for computing the response coefficients in stochastic finite element analysis", *Proc. AsRANET 2*, Barcelona, Spain, 2004a.
- Berveiller M., Sudret B., Lemaire M., "Presentation of two methods for computing the response coefficients in stochastic finite element analysis", *Proc. 9th ASCE specialty Conference on Probabilistic Mechanics and Structural Reliability*, Albuquerque, USA, 2004b.
- Berveiller M., Sudret B., Lemaire M., "Non linear non intrusive stochastic finite element method - Application to a fracture mechanics problem", in , G. Augusti, , G. Schuëller, , M. Ciampoli (eds), *Proc. 9th Int. Conf. Struct. Safety and Reliability (ICOSSAR'2005)* Roma, Italie, Millpress, Rotterdam, 2005.
- Berveiller M., Sudret B., Lemaire M., "Stochastic finite element : a non intrusive approach by regression", *Revue Européenne de Mécanique Numérique*, vol. 15, n° 1-3, p. 81-92, 2006.
- Choi S., Grandhi R., Canfield R., "Structural reliability under non-Gaussian stochastic behavior", *Computers and Structures*, vol. 82, 2004a, p. 1113-1121.
- Choi S., Grandhi R., Canfield R., Pettit C., "Polynomial Chaos Expansion with Latin Hypercube Sampling for Estimating Response Variability", *AIAA Journal*, vol. 45, 2004b, p. 1191-1198.
- Deb M., Babuska I., Oden J., "Solution of stochastic partial differential equations using Galerkin finite element techniques", *Comp. Meth. Appl. Mech. Eng.*, vol. 190, n° 48, 2001, p. 6359-6372.
- Deodatis G., "The weighted integral method, I : stochastic stiffness matrix", *J. Eng. Mech.*, vol. 117, n° 8, 1991, p. 1851-1864.
- Deodatis G., Shinozuka M., "The weighted integral method, II : response variability and reliability", *J. Eng. Mech.*, vol. 117, n° 8, 1991, p. 1865-1877.
- Der Kiureghian A., Ke J.-B., "The stochastic finite element method in structural reliability", *Prob. Eng. Mech.*, vol. 3, n° 2, 1988, p. 83-91.
- Der Kiureghian A., Liu P.-L., "Structural reliability under incomplete probability information", *J. Eng. Mech., ASCE*, vol. 112, n° 1, 1986, p. 85-104.
- Der Kiureghian A., Taylor R.-L., "Numerical methods in structural reliability", *Proc. 4th Int. Conf. on Appl. of Statistics and Probability in Soil and Structural Engineering*, 1983, p. 769-784.
- Det Norske Veritas, *PROBAN user's manual, V.4.3*, 2000.
- Ditlevsen O., Madsen H., *Structural reliability methods*, J. Wiley and Sons, Chichester, 1996.
- Field R., Grigoriu M., "On the accuracy of the polynomial approximation", *Prob. Eng. Mech.*, vol. 19, 2004, p. 65-80.
- Frangopol D., Imaia K., "Geometrically nonlinear finite element reliability analysis of structural systems. II: applications", *Comput. Struc.*, vol. 77, n° 6, 2000, p. 693-709.

- Frangopol D.M., Maute K. (Editors), "Advances in Probabilistic Mechanics and Structural Reliability", *Comput. Struct.*, 2004.
- Ghanem R., "Probabilistic characterization of transport in heterogeneous media", *Comp. Meth. Appl. Mech. Eng.*, vol. 158, 1998, p. 199-220.
- Ghanem R., "Ingredients for a general purpose stochastic finite elements implementation", *Comp. Meth. Appl. Mech. Eng.*, vol. 168, 1999a, p. 19-34.
- Ghanem R., "Stochastic finite elements with multiple random non-Gaussian properties", *J. Eng. Mech., ASCE*, vol. 125, n° 1, 1999b, p. 26-40.
- Ghanem R., "Iterative solution of systems of linear equations arising in the context of stochastic finite elements", *Advances in Engineering Software*, vol. 31, 2000, p. 607-616.
- Ghanem R., Kruger R., "Numerical solution of spectral stochastic finite element systems", *Comp. Meth. Appl. Mech. Eng.*, vol. 129, n° 3, 1996, p. 289-303.
- Ghanem R., Spanos P., *Stochastic finite elements - A spectral approach*, Springer Verlag, 1991.
- Ghanem R., Spanos P.-D., "Polynomial chaos in stochastic finite elements", *J. App. Mech., ASME*, vol. 57, 1990, p. 197-202.
- Ghiocel D., Ghanem R., "Stochastic finite element analysis of seismic soil-structure interaction", *J. Eng. Mech., (ASCE)*, vol. 128, 2002, p. 66-77.
- Hisada T., Nakagiri S., "Stochastic finite element method developed for structural safety and reliability", *Proc. 3rd Int. Conf. Struct. Safety and Reliability, ICOSSAR'81*, 1981, p. 395-408.
- Hisada T., Nakagiri S., "Role of stochastic finite element method in structural safety and reliability", *Proc. 4th Int. Conf. Struct. Safety and Reliability, ICOSSAR'85*, 1985, p. 385-395.
- Imaia K., Frangopol D., "Geometrically nonlinear finite element reliability analysis of structural systems. I: theory", *Comput. Struc.*, vol. 77, n° 6, 2000, p. 677-691.
- Isukapalli S. S., *Uncertainty Analysis of Transport-Transformation Models*, PhD thesis, The State University of New Jersey, 1999.
- Keese A., Matthies H., "Efficient solvers for non linear stochastic problems", H. Mang, , F. Rammerstorfer, , J. Eberhardsteiner (eds), *Proc. 5th World Cong. Comp. Mech.*, 2002.
- Kleiber, M. (Editor), "Computational stochastic mechanics", *Comp. Meth. Appl. Mech. Eng.*, 1999.
- Kleiber M., Hien T.-D., *The stochastic finite element methods - Basic perturbation technique and computational implementation*, J. Wiley and sons, Chichester, 1992.
- Lemaire M., "Finite element and reliability : combined methods by surface response", G.N. Frantziskonis (ed.), *Probamat-21st Century, Probabilities and Materials : Tests, Models and Applications for the 21st century*, Kluwer Academic Publishers, 1998, p. 317-331.
- Lemaire M., Mohamed A., "Finite Element and Reliability: A Happy Marriage?", *Proc. 9th IFIP WG 7.5 Working Conference on Reliability and Optimization of Structural Systems (Keynote lecture)*, Nowak A. and Szerszen M., 2000, p. 3-14.
- Li C., Der Kiureghian A., "Optimal discretization of random fields", *J. Eng. Mech.*, vol. 119, n° 6, 1993, p. 1136-1154.
- Liu W., Belytschko T., Mani A., "Probabilistic finite elements for non linear structural dynamics", *Comp. Meth. App. Mech. Eng.*, vol. 56, 1986a, p. 61-86.

- Liu W., Belytschko T., Mani A., "Random field finite elements", *Int. J. Num. Meth. Eng.*, vol. 23, n° 10, 1986b, p. 1831-1845.
- Malliavin P., *Stochastic Analysis*, Springer, 1997.
- Mathworks T., *Manuel de référence du logiciel Matlab*, 2001.
- Matthies G., Brenner C., Bucher C., Guedes Soares C., "Uncertainties in probabilistic numerical analysis of structures and solids - Stochastic finite elements", *Struct. Safety*, vol. 19, n° 3, 1997, p. 283-336.
- Mohamed A., Pendola M., Heinfling G., Defaux G., "Etude de l'intégrité des aéro-réfrigérants par couplage éléments finis et fiabilité", *Revue Européenne des Eléments Finis*, vol. 1, 2002, p. 101-126.
- Pendola M., Mohamed A., Lemaire M., Hornet P., "Combination of finite element and reliability methods in nonlinear fracture mechanics", *Reliability Engineering & System Safety*, vol. 70, n° 1, 2000, p. 15-27.
- Puig B., Poirion F., Soize C., "Non-Gaussian simulation using Hermite polynomial expansion: convergences", *Prob. Eng. Mech.*, vol. 17, 2002, p. 253-264.
- Schuëller, G. (Editor), "A state-of-the-art report on computational stochastic mechanics", *Prob. Eng. Mech.*, 1997. IASSAR report.
- Sudret B., "Des éléments finis stochastiques spectraux aux surfaces de réponse stochastiques : une approche unifiée", *Proc. 17e Congrès Français de Mécanique - Troyes*, 2005.
- Sudret B., Berveiller M., Lemaire M., "Application of a Stochastic Finite Element Procedure to Reliability Analysis", *Proc 11th IFIP WG7.5 Conference on Reliability and Optimization of Structural Systems, Banff, Canada*, 2003, p. 319-327.
- Sudret B., Berveiller M., Lemaire M., "Eléments finis stochastiques en élasticité linéaire", *C. R. Mécanique*, vol. 332, 2004, p. 531-537.
- Sudret B., Defaux G., Pendola M., "Time-variant finite element reliability analysis - application to the durability of cooling towers", *Struct. Safety*, vol. 27, 2005, p. 93-112.
- Sudret B., Der Kiureghian A., Stochastic finite elements and reliability : A state-of-the-art report, Technical Report n° UCB/SEMM-2000/08, University of California, Berkeley, 2000. 173 pages.
- Sudret B., Der Kiureghian A., "Comparison of finite element reliability methods", *Prob. Eng. Mech.*, vol. 17, 2002, p. 337-348.
- Takada T., "Weighted integral method in multidimensional stochastic finite element analysis", *Prob. Eng. Mech.*, vol. 5, n° 4, 1990a, p. 158-166.
- Takada T., "Weighted integral method in stochastic finite element analysis", *Prob. Eng. Mech.*, vol. 5, n° 3, 1990b, p. 146-156.
- Van Den Nieuwenhof B., Coyette J.-P., "Modal approaches for the stochastic finite element analysis of structures with material and geometric uncertainties", *Comp. Meth. Appl. Mech. Eng.*, vol. 192, n° 33-34, 2003, p. 3705-3729.
- Webster M., Tatang M., McRae G., Application of the Probabilistic Collocation Method for an Uncertainty Analysis of a Simple Ocean Model, Technical report, MIT Joint Program on the Science and Policy of Global Change Reports Series No. 4, Massachusetts Institute of Technology, 1996.
- Xiu D., Karniadakis G. E., "The Wiener-Askey polynomial chaos for stochastic differential equations", *J. Sci. Comput.*, vol. 24, n° 2, 2002, p. 619-644.

- Xiu D., Karniadakis G. E., “A new stochastic approach to transient heat conduction modeling with uncertainty”, *Int. J. Heat Mass Transfer*, vol. 46, 2003, p. 4681-4693.
- Yu Y., Coupling a Stochastic Finite element Solver with ANSYS and Visualization of the Results, Technical Report n° Matr.-Nr.: 2663324, Institute of scientific Computing, Technische Universität Carolo-Wilhelmina zu Braunschweig, 2003.
- Zhang J., Ellingwood B., “Orthogonal series expansion of random fields in reliability analysis”, *J. Eng. Mech., ASCE*, vol. 120, n° 12, 1994, p. 2660-2677.
- Zienkiewicz O.-C., Taylor R.-L., *The finite element method*, Butterworth Heinemann, 5th edition, 2000.

Appendix I: description of the polynomial chaos and implementation

Introduction and notation

Let us denote by $\mathcal{L}^2(\Theta, F, P)$ the Hilbert space of random variables with finite variance. $\{H_i, i = 0, \dots, \infty\}$ are Hermite polynomials defined by:

$$H_i(x) = (-1)^i \frac{1}{\varphi(x)} \frac{d^i \varphi(x)}{dx^i} \tag{77}$$

where $\varphi(x) = \frac{1}{\sqrt{2\pi}} e^{-\frac{x^2}{2}}$. The set $\{H_i, i = 0, \dots, \infty\}$ is an orthogonal basis of the Hilbert space $\mathcal{L}^2(\varphi)$ of the square integrable functions with respect to the Gaussian measure (Malliavin, 1997):

$$\frac{dH_n(x)}{dx} = n H_{n-1}(x) \tag{78}$$

and:

$$H_i(x) H_j(x) = \sum_{k \geq 0} C_{ijk} H_k(x) \tag{79}$$

with:

$$C_{ijk} = \begin{cases} \frac{i!j!}{\left(\frac{i+j-k}{2}\right)! \left(\frac{j+k-i}{2}\right)! \left(\frac{k+i-j}{2}\right)!} & \text{if } \begin{cases} (i+j+k) \text{ even} \\ k \in [|i-j|, i+j] \end{cases} \\ 0 & \text{otherwise} \end{cases} \tag{80}$$

Using these properties, deriving the expectation of products of two, three or four Hermite polynomials of a standard normal variable ξ is straightforward:

$$D_{ij} = E[H_i(\xi)H_j(\xi)] = \delta_{ij}j! \tag{81}$$

where δ_{ij} is the Kronecker symbol.

$$D_{ijk} = E[H_i(\xi)H_j(\xi)H_k(\xi)] = \begin{cases} \frac{i!j!k!}{\left(\frac{i+j-k}{2}\right)!\left(\frac{j+k-i}{2}\right)!\left(\frac{k+i-j}{2}\right)!} & \text{if } \begin{cases} (i+j+k) \text{ even} \\ k \in [|i-j|, i+j] \end{cases} \\ 0 & \text{otherwise} \end{cases} \quad [82]$$

and finally:

$$D_{ijkl} = E[H_i(\xi)H_j(\xi)H_k(\xi)H_l(\xi)] = \sum_{q \geq 0} D_{ijq} C_{klq} \quad [83]$$

Let us denote by $\{\xi_i\}_{i=1}^M$ M standard normal variables and by $\{\Psi_j\}$ the so-called *polynomial chaos basis*. The M -th dimensional p -th order polynomial is the set of multidimensional Hermite polynomials in $\{\xi_i\}_{i=1}^M$, whose degree does not exceed p . Each polynomial is completely defined by a sequence of M non-negative integers $\alpha = \{\alpha_1, \dots, \alpha_M\}$ (whose sum is smaller or equal than p):

$$\Psi_\alpha = \prod_{i=1}^M H_{\alpha_i}(\xi_i) \quad , \quad \alpha_i \geq 0 \quad [84]$$

Let us denote by $\partial_\alpha = \sum_{i=1}^M \alpha_i$ the degree of the sequence α . The implementation of the polynomial chaos requires:

- computing and storing the coefficients of the one-dimensional Hermite polynomials (Equation [78]);
- generating all sequences α , whose degree is less or equal to p . These sequences are labeled from 0 to $P - 1$ and the corresponding polynomials are denoted by $\{\Psi_j, j = 0, \dots, P - 1\}$.

Implementation of the polynomial chaos basis

For each degree $q = \{1, \dots, p\}$, the goal is to compute all sequences of M non negative integers whose sum equals q . This problem is equivalent to that of filling $(M + q - 1)$ boxes with $(M - 1)$ balls (Figure 10), see also (Sudret *et al.*, 2000). The correspondence between the integer sequence and the box samples is described below:

- for each integer α_i of the sequence, skip α_i empty boxes and put a ball in the next one;

– conversely, for each ball sample, each integer α_i of the sequence equals the number of empty boxes (possibly 0) between two consecutive balls.

From this equivalence, the number of sequences α of degree $\partial_\alpha = q$ is the number of corresponding ball samples, *i.e.* the binomial factor $\binom{M+q-1}{M-1} = \binom{M+q-1}{q}$.



ball sample	integer sequence	Polynomial basis
	1 0 1 0	$H_1(\xi_1) \cdot H_1(\xi_3) = \xi_1 \xi_3$
	0 0 0 2	$H_2(\xi_4) = \xi_4^2 - 1$

Figure 10. Equivalence of the balls samples and the integers sequence α for $(M = 4, p = 2)$

The algorithm which generates all filling of $(M + q - 1)$ boxes with $(M - 1)$ ball in the case $(q = 2, M = 4)$ is described in Figure 11 and reads as follows (note that only polynomials of degree 2 are represented):

– for a given q , the initial sample is obtained by putting all balls in the $(M - 1)$ first boxes and corresponds to the sequence $\alpha = \{0, \dots, 0, q\}$.

– from the current sample, the next one is recursively obtained by shifting the rightmost ball by one box to the right. If this is not possible (*i.e.* the right most ball is already in the rightmost box), then the rightmost ball that can be shifted by one box to the right is found. This ball is shifted, and all the balls lying to its right are brought back to its immediate left.

Note that, for each degree q , the integer sequences are labeled in reverse order in order to get the Ψ_j basis in the same order as that originally presented in (Ghanem *et al.*, 1991). The number of polynomials in M variables having a degree lower than or equal to p is given by:

$$P = \sum_{k=0}^p \binom{M+k-1}{k} \tag{85}$$

Expectation of products of Hermite polynomials

By extension of Equation [81], the polynomials $\{\Psi_j, j = 0, \dots, P - 1\}$ are orthogonal and satisfy:

$$E[\Psi_\alpha \cdot \Psi_\beta] = \delta_{\alpha\beta} \cdot \prod_{i=1}^M \alpha_i! \tag{86}$$











ball sample	integer sequence	Reverse order	Polynomial basis
	0 0 0 2	2 0 0 0	$\xi_1^2 - 1$
	0 0 1 1	1 1 0 0	$\xi_1 \xi_2$
	0 0 2 0	1 0 1 0	$\xi_1 \xi_3$
	0 1 0 1	1 0 0 1	$\xi_1 \xi_4$
	0 1 1 0	0 2 0 0	$\xi_2^2 - 1$
	0 2 0 0	0 1 1 0	$\xi_2 \xi_3$
	1 0 0 1	0 1 0 1	$\xi_2 \xi_4$
	1 0 1 0	0 0 2 0	$\xi_3^2 - 1$
	1 1 0 0	0 0 1 1	$\xi_3 \xi_4$
	2 0 0 0	0 0 0 2	$\xi_4^2 - 1$

Figure 11. Recursive generation of the polynomial chaos ($q = 2, M = 4$)

where $\delta_{\alpha\beta}$ is the Kronecker symbol, whose value is 1 if sequences α and β are identical and 0 otherwise.

In Equation [39], the expectation of three polynomials is needed. Following Equation [84], let us denote:

$$\left\{ \begin{array}{l} \Psi_i = \prod_{m=1}^M H_{\alpha_m}(\xi_m) \quad , \quad \alpha_m \geq 0 \\ \Psi_j = \prod_{m=1}^M H_{\beta_m}(\xi_m) \quad , \quad \beta_m \geq 0 \\ \Psi_k = \prod_{m=1}^M H_{\gamma_m}(\xi_m) \quad , \quad \gamma_m \geq 0 \end{array} \right. \quad [87]$$

where $\{\alpha_1, \dots, \alpha_M\}, \{\beta_1, \dots, \beta_M\}, \{\gamma_1, \dots, \gamma_M\}$ denote M non-negative integer sequences. From Equations [82],[87], it comes:

$$d_{ijk} = E[\Psi_i \Psi_j \Psi_k] = \prod_{m=1}^M D_{\alpha_m \beta_m \gamma_m} \quad [88]$$

Similarly, the expectation of products of four multi-dimensional Hermite polynomials used in Equation [58] is:

$$d_{ijkl} = E[\Psi_i \Psi_j \Psi_k \Psi_l] = \prod_{m=1}^M D_{\alpha_m \beta_m \gamma_m \delta_m} \tag{89}$$

where $D_{\alpha_m \beta_m \gamma_m \delta_m}$ is given in Equation [83].

The Matlab implementation of the polynomial chaos as described above can be download for free at: [<http://www.ce.berkeley.edu/haukaas/FERUM/ferum.html>]

Appendix II: positioning of coefficients in the polynomial chaos basis

Let us denote by $\{X^1, \dots, X^M\}$ M independent random variables expanded separately onto the Hermite polynomial basis of standard normal random variables $\{\xi_1, \dots, \xi_M\}$ at the order n_i , $i = \{1, \dots, M\}$:

$$X^i = \sum_{k=0}^{n_i} x_k^i H_k(\xi_i) \tag{90}$$

Input

. (x_k^i) $i = \{1, \dots, M\}$, $k = \{0, \dots, n_i\}$

Initialisation

. $\tilde{x}_0^i = x_0^i$ $i = \{1, \dots, M\}$

. $\tilde{x}_j^i = 0$ $i = \{1, \dots, M\}$ $j = \{1, \dots, P - 1\}$

Positioning

. for $j = \{1, \dots, P - 1\}$

. if α_j has only one non zero term $\alpha_j(q)$ at q -th position:

. if $\alpha_j(q) \leq n_q$ then $\tilde{x}_j^q = x_{\alpha_j(q)}^q$

. end if

. end for j

Figure 12. Positioning algorithm for injection Hermite series expansion into the polynomial chaos

These variables can be expanded onto the polynomial chaos basis of degree $p = \max_{i=1, \dots, M} n_i$ as follows:

$$X^i = \sum_{j=0}^{P-1} \tilde{x}_j^i \Psi_j(\{\xi_k\}_{k=1}^M) \tag{91}$$

where P is related to p and M by Equation [85]. The positioning consists in establishing the correspondence between \tilde{x}_j^i and x_k^i . For each variable X^i , the coefficient of order 0 (the mean value) is the same in both basis. Moreover, all coefficients \tilde{x}_j^i corresponding to a truly multidimensional polynomial Ψ_j (*i.e.*, Ψ_j depends on more than one variable ξ_k) are zero. Thus the positioning algorithm described in Figure 12.